Geomechanics and Engineering, *Vol. 24, No. 3 (2021) 267-280*
DOI: https://doi.org/10.12989/gae.2021.24.3.267

Dynamic stability analysis of a rotary GPLRC disk surrounded by viscoelastic foundation

Xiujuan Liang[a] and Haixu Ji*

School of Mechanical and Power Engineering, Guangdong Ocean University, Zhanjiang 524008, Guangdong, China

(Received July 20, 2020, Revised January 20, 2021, Accepted January 21, 2021)

Abstract. The research presented in this paper deals with dynamic stability analysis of the graphene nanoplatelets (GPLs) reinforced composite spinning disk. The presented small-scaled structure is simulated as a disk covered by viscoelastic substrate which is two-parametric. The centrifugal and Coriolis impacts due to the spinning are taken into account. The stresses and strains would be obtained using the first-order-shear-deformable-theory (FSDT). For Poisson ratio, as well as various amounts of mass densities, the mixture rule is employed, while a modified Halpin-Tsai model is inserted for achieving the elasticity module. The structure's boundary conditions (BCs) are obtained employing GPLs reinforced composite (GPLRC) spinning disk's governing equations applying principle of Hamilton which is based on minimum energy and ultimately have been solved employing numerical approach called generalized-differential quadrature-method (GDQM). Spinning disk's dynamic properties with different boundary conditions (BCs) are explained due to the curves drawn by Matlab software. Also, the simply-supported boundary conditions is applied to edges $\theta=\pi/2$, and $\theta=3\pi/2$, while, cantilever, respectively, is analyzed in $R=R_i$, and R_0. The final results reveal that the GPLs' weight fraction, viscoelastic substrate, various GPLs' pattern, and rotational velocity have a dramatic influence on the amplitude, and vibration behavior of a GPLRC rotating cantilevered disk. As an applicable result in related industries, the spinning velocity impact on the frequency is more effective in the higher radius ratio's amounts.

Keywords: GPLRC 2-D cantilevered disk; viscoelastic foundation; rotation; FSDT; finite element approach; numerical model; dynamic stability

1. Introduction

Nowadays, reinforcements of GPLs has been attracted by a lot of researchers due to improvement in the mechanical characterizations (Jafari Fesharaki and Roghani 2019), owing to its boosted the thermal conductivity, along with flame retardant. Dynamic stability analysis of structure has been attracted a lot of attention (Zuo *et al.* 2013, Liu *et al.* 2015, Pang *et al.* 2018, Zhu *et al.* 2018, Abedini *et al.* 2019, Zhang *et al.* 2019a, Alam *et al.* 2020a, Liu *et al.* 2020a, b, c, d, Wang *et al.* 2020, Yang *et al.* 2020, Zhang *et al.* 2020a, b, Zhu *et al.* 2020). Gholami *et al.* (Gholami and Ansari 2019) reported GPLRC plate's nonlinear frequency analysis applying higher-order shear deformation theory (HSDT). They, however, solved the governing motion equations through multistep computational model (Abedini and Zhang 2020, Cao 2020, Liu *et al.* 2020e, Mousavi *et al.* 2020, Zhang *et al.* 2020). The sandwich plate's forced and Free vibration considering core of viscoelasticity which is combined by layers of GPLRC have been investigated by Ref. (Mohseni and Shakouri 2020). Employing classical theory and energy approach, the researchers obtained the governing motion equations and ultimately Navier approach has been used to solve them precisely. GPLRC microplate's frequency investigation employing a small-scaled model and considering analytical approach has been firstly presented by Mohammad-Rezaei Bidgoli *et al.* (2019). A considerable outcome was that arrange of factors of size–dependent elements has dramatically contributed in the GPLRC microplate's frequency characteristics. The low velocity influence on the GPLRC plate's deflection considering imperfected configuration was reported by Ref. (Song *et al.* 2019). They applied mixture approach as well as Halpin-Tsai for computing the elasticity module along with other material properties. GPLRC plate's resonance behavior employing Navier method (Abedini *et al.* 2020b, Kordestani *et al.* 2020, Xu *et al.* 2020, Zhang *et al.* 2020d) has been scrutinized by Ref (Karami *et al.* 2019). They have simulated the GPLRC plate through using Kirchhoff plate model and associated BCs and governing equations have been determined by principle of minimum energy. In the mentioned research they have demonstrated that the impact of layers' number on their structure's stability has not that depended on the types of GPLs. Moreover, GPLRC plate's natural frequency investigation using computational solution approach has been reported by Gunasekaran *et al.* (2020). Using FEM, GPLRC curved plate's forced vibration (Zhang *et al.* 2020e) performances subjected to high-temperature situation (Cui *et al.*) has been introduced by Re. (Tran *et al.* 2020). A prominent outcome that they disclosed in their research was that GPLs' configurational characters have a dramatic impact on the curved GPLRC

*Corresponding author, Ph.D.
E-mail: liangxj12345@163.com
[a]Ph.D.
E-mail: liangxj@gdou.edu.cn

ISSN: 2005-307X (Print), 2092-6219 (Online)

plate's resonance. In addition, GPLRC curved sector plate's critical temperature considering a nonlinearity known as von Kármán model and first-order-shear-deformation model has been reported by Javani *et al.* (2020). They have employed GDQM and eventually disclosed that by using GPLs' small amount into the matrix, crucial temperature tends to be raised. This kind of structure can be used in many systems (Sun *et al.* 2019, Wang *et al.* 2020b) such as concrete (Zhang *et al.* 2019b, Abedini and Zhang 2020c, Alam *et al.* 2020b, Ju *et al.* 2020, Sun *et al.* 2020, Wu *et al.* 2021) in various conditions via experimental date (Alam *et al.* 2020c, Huang *et al.* 2020, Li *et al.* 2020, Zheng *et al.* 2020f). It is uncovered that circular plates would be applied in multifarious engineering and industrial applications (Bai *et al.* 2020). Due to different dynamic and static forces that would drop the system's stability (Long *et al.* 2015, Xiong *et al.* 2016, Wu *et al.* 2019, Zhang and Wang 2019c, d, Dong *et al.* 2020, Zhang and Wang 2020g, Dong and Cui 2021), the presented structure is usually is subjected to a wide range of environment situations. As well as this, undesirable performances would happen for the mentioned structures including cracks, buckling, resonance and deformations. Then, it would be highly important for designers to understand the mechanical performances of this system type for analyzing the structure considering a significant reliability. Due to the GRLs reinforcements' benefits, this class of material would be applied as a composite filler (Zhu *et al.* 2018) in the circular plates. Employing 3D-elasticity model, Yang *et al.* (2017) scrutinized circular/annular plate's bending investigation. They. However, disclosed that distribution pattern, BCs, and other configurational and physical factors of the GPLs have vital contributions in the structure's strain and stress fields. GPLRC annular plate's bending and Frequency characteristics employing 3D-elasticity model have been evaluated by Liu *et al.* (2019). They have solved the system's governing motion equations via state-space based DQM. They uncovered that a range of BCs, and other structure's physical and geometrical factors and GPLs have been playing a prominent role in the GPLRC annular plate's bending and Frequency characteristics. GPLRC circular plate's nonlinear forced vibration in an extreme temperature situation has been reported by Wu *et al.* (Wu, Zhu *et al.* 2020). Using iterative approach and GDQM, they solved the nonlinear governing motion equations considering related BCs. Eventually, they demonstrated that the ratio of nonlinear frequency drops when GPL fillers increases within the GPLRC circular plate's outer layers. Spinning disks, plates and have a broad range of applications including, compressors, computer disks, pump, and rotors., In the area of spinning circular/annular plate's instability/stability investigation, Hu *et al.* (2016) analyzed rotating circular plate's nonlinear performance subjected to magnetic field. The structure presented by them was simulated via thin plate model and ultimately they have solved the nonlinear governing motion equations through using multiple scales and Galerkin approaches. They disclosed that, rotational speed, and magnetic excitation have an important contribution in the rotating circular plate's instability/stability. Ref. (Bagheri *et al.* 2019) dealt with stability study of a rotating homogeneous isotropic annular plate. By applying von Kármán nonlinearity and FSDT, the model was derived. Mahinzare *et al.* (2018) evaluated functionally graded (FG) spinning circular plate's frequency characteristics using a classical model, while governing motion equations have been solved via DQM. They, however, demonstrated that related factors to FG, angular speed, and external voltage have a significant contribution in the smart (FG) circular plate's frequency behavior. Furthermore, Qin *et al.* (2018) studied cylindrical shell's vibrational performances coupled with circular disk within framework of Rayleigh–Ritz approach. Recently, hygro-thermal environment's impact of the magneto-electro-elastic (MEE) imperfect circular plate's multi-field responses has been reported by Ref. (Dai *et al.* 2019). the thermal situation has been created using a steady-state heat conduction. Ultimately, the governing equation has been solved via DQM, then the outcomes revealed the external conditions' impacts (extreme temperature and moisture) on the imperfected annular MEE plate's multi-field responses. Refs. (El-Hassar *et al.* 2016, Fahsi *et al.* 2017, Issad *et al.* 2018, Sadoun *et al.* 2018, Younsi *et al.* 2018, Ahmed *et al.* 2019, Boulefrakh *et al.* 2019, Chikr, Kaci *et al.* 2020, Rabhi *et al.* 2020), however, reported structures' instability/stability investigation considering a wide range of solution approaches (Ghabussi *et al.* 2019, Habibi *et al.* 2019, Al-Furjan *et al.* 2020a, b, c, d, e, f, g, h, i, j, k, l, m, Ebrahimi *et al.* 2020, Habib *et al.* 2020, Lori *et al.* 2020, Moayedi *et al.* 2020, Safarpour *et al.* 2020, Shokrgozar *et al.* 2020). The bi-axial micro-scanner's instability investigation which is subjected to electromagnetic actuation such as size dependency and damping impacts has been studied by Ref. (Atabak *et al.* 2020). stress-based non-local elasticity for the fluid-conveying C-BN hybrid-nanotube's instability located in a magneto-thermal situation has been scrutinized by Sedighi *et al.* (Sedighi *et al.* 2020a). In their research, the size dependency had been considered employing Eringen's strain-based non-local differential theory. hetero-nanotube's dynamics made of boron nitride (BN) and carbon (C) nanotubes in thermal and magnetic situation applying a FE model has been reported by Ref. (Sedighi *et al.* 2020b). Lately, Safarpour *et al.* (2019) have studied frequency, and bending information of cylindrical shell, truncated GPLRC conical shell, and circular plate through using DQM and three-dimensional model of elasticity. Then, it found that GPLs' pattern types, GPLs', weight fraction, configurational factors including ratio of length to mid-radius and semi-vertex angle have vital contributions in the GPLRC structures' bending, and frequency. They (Bisheh *et al.* 2019), moreover, analyzed FG- annular and circular GPLRC plate's bending and natural frequencies considering a range of BCs. They derived and solved, respectively, the annular and circular FG-GPLRC plate's governing equations applying three-dimensional elasticity model, and DQM. To the best of aforementioned scientists' knowledge, spinning cantilevered GPLRC disk's frequency and amplitude information which is covered by viscoelastic substrate have not been reported in the aforementioned literature. In the present study, modified Halpin-Tsai's micromechanics is

employed for approximating effective elastic properties. Furthermore, a computational approach is applied to solve governing motion equations and derived via principle of minimum energy. Despite semi-computational solution, an FE method has been introduced applying the FE package for simulating the spinning cantilevered GPLRC disk's response. The outcomes derived by the FE simulation demonstrates a close agreement with the results of semi-computational approach. A significant attention is given for analyzing some physical and configurational factors' impacts on the frequency, and amplitude behaviors of a spinning cantilevered GPLRC disk covered by viscoelastic substrate.

2. The mathematical formulations for spinning GPLRC cantilevered disk

A rotating GPLRC cantilevered microdisk surrounded by viscoelastic foundation is shown in Fig. 1.

Four patterns have been considered for modelling GPLRC reinforcements, in the current manuscript. The functions of volume fraction are defined for each figure as follows (Song *et al.* 2017):

$$V_{GPL}(k) = V_{GPL}^{*} \quad U-GPLRC \tag{1}$$

$$V_{GPL}(k) = 2\left|2k - N_L - 1\right| V_{GPL}^{*} / N_L \quad X-GPLRC \tag{2}$$

$$V_{GPL}(k) = 2(2k-1)V_{GPL}^{*} / N_L \quad A-GPLRC \tag{3}$$

$$V_{GPL}(k) = 2\left[1-\left(\left|2k - N_L - 1\right| / N_L\right)\right]V_{GPL}^{*} \quad O-GPLRC \tag{4}$$

Ref (Song *et al.* 2017) provides us with details of factors applied in Eqs. (1)-(4). The dependence of $\mathbf{V_{GPL}^{*}}$ and its weight fraction g_{GPL} may be explained by:

$$V_{GPL}^{*} = \frac{g_{GPL}}{g_{GPL} + (\rho_{GPL} / \rho_m)(1 - g_{GPL})} \tag{5}$$

Here the mass density of GPL and polymer matrix are depicted as $\boldsymbol{\rho_{GPL}}$ and $\boldsymbol{\rho_m}$ respectively. The GPLRC shell's elasticity modulus has been supposed using modified Halpin-Tsai micro-sized mechanics (De Villoria and Miravete 2007)

$$E = \left(\frac{3}{8}\left(\frac{1+\xi_L \eta_L V_{GPL}}{1-\eta_L V_{GPL}}\right) + \frac{5}{8}\left(\frac{1+\xi_W \eta_W V_{GPL}}{1-\eta_W V_{GPL}}\right)\right) \times E_M$$

$$\xi_L = 4L_{GPL} / 2t_{GPL} \quad \xi_W = (4\, w_{GPL} / 2t_{GPL})$$

$$\eta_L = (-E_M + E_{GPL}) / (\xi_L E_M + E_{GPL}) \tag{6}$$

$$\eta_W = (-1 + \frac{E_{GPL}}{E_M}) \Big/ (\xi_W + \frac{E_{GPL}}{E_M})$$

Eventually, Poisson's ratio ν_c are defined as below by applying the rule of mixture and polymer micro GNP composite's density ρ_c:

$$\nu = \nu_{GPL} V_{GPL} + \nu_M V_M,$$
$$\rho = \rho_{GPL} V_{GPL} + \rho_M V_M. \tag{7}$$

2.1 Disk's displacement fields

The fields of displacement would be expressed by the below equations, according to FSDT:

$$u(R,\beta,z,t) = u_0(R,\beta,t) + z u_1(R,\beta,t)$$
$$v(R,\beta,z,t) = v_0(R,\beta,t) + z v_1(R,\beta,t) \tag{8}$$
$$w(R,\beta,z,t) = w_0(R,\beta,t)$$

2.2 Strain-stress of the structure

The strain- stress relations would be explained as below, according to the FSDT:

$$\begin{bmatrix} \sigma_{xx} \\ \sigma_{\theta\theta} \\ \sigma_{x\theta} \\ \sigma_{xz} \\ \sigma_{\theta z} \end{bmatrix} = \begin{bmatrix} Q_{11} & Q_{12} & 0 & 0 & 0 \\ Q_{21} & Q_{22} & 0 & 0 & 0 \\ 0 & 0 & Q_{66} & 0 & 0 \\ 0 & 0 & 0 & Q_{55} & 0 \\ 0 & 0 & 0 & 0 & Q_{44} \end{bmatrix} \begin{bmatrix} \varepsilon_{xx} \\ \varepsilon_{\theta\theta} \\ \varepsilon_{x\theta} \\ \varepsilon_{xz} \\ \varepsilon_{\theta z} \end{bmatrix} \tag{9}$$

$$Q_{11} = Q_{22} = \frac{\bar{E}}{1-\bar{\nu}^2}, \; Q_{12} = Q_{21} = \frac{\bar{E}\bar{\nu}}{1-\bar{\nu}^2}, \quad Q_{44} = Q_{55} = Q_{66} = \frac{\bar{E}}{2(1+\bar{\nu})}$$

Then, the components of strain may be calculated as (Hosseini-Hashemi *et al.* 2010, Ghiasian *et al.* 2014):

$$\begin{Bmatrix} \varepsilon_{RR} \\ \varepsilon_{\beta\beta} \\ \gamma_{R\beta} \\ \gamma_{Rz} \\ \gamma_{\beta z} \end{Bmatrix} = \begin{bmatrix} \frac{\partial u}{\partial R} = \left(\frac{\partial u_0}{\partial R} + z\frac{\partial u_1}{\partial R}\right) \\ \frac{\partial v}{R\partial\beta} + \frac{u}{R} = \left(\frac{\partial v_0}{R\partial\beta} + z\frac{\partial v_1}{R\partial\beta} + \frac{u_0}{R} + z\frac{u_1}{R}\right) \\ \frac{\partial v}{\partial R} + \frac{1}{R}\frac{\partial u}{\partial\beta} - \frac{1}{R}v = \left(\frac{\partial v_0}{\partial R} + z\frac{\partial v_1}{\partial R} + \frac{1}{R}\frac{\partial u_0}{\partial\beta} + \frac{z}{R}\frac{\partial u_1}{\partial\beta} - \frac{1}{R}v_0 - z\frac{v_1}{R}\right) \\ \frac{\partial u}{\partial z} + \frac{\partial w}{\partial R} = \left(u_1 + \frac{\partial w_0}{\partial R}\right) \\ \frac{\partial v}{\partial z} + \frac{1}{R}\frac{\partial w}{\partial\beta} = \left(v_1 + \frac{1}{R}\frac{\partial w_0}{\partial\beta}\right) \end{bmatrix} \tag{10}$$

2.3 Extended Hamilton's principle

Relations between motion equations and BCs would be defined as the following equations, according to the principle of minimum energy (Sedighi and Daneshmand 2014, Ouakad and Sedighi 2019, Al-Furjan *et al.* 2020n, o, p, q, Moraveji Tabasi *et al.* 2020, Wang *et al.* 2020c, Al-Furjan *et al.* 2021):

$$\int_{t_1}^{t_2} (\delta T - \delta U + \delta W)\, dt = 0 \tag{11}$$

Spinning disk's Speed vectors would be defined as

below (Hu and Wang 2016, Hu and Li 2019):

$$\left(\frac{\partial u}{\partial t}-\Omega v\right)i+\left(\frac{\partial u}{\partial t}+\Omega(R+u)\right)j+\left(\frac{\partial w}{\partial t}\right)k \tag{12}$$

I would be important to mention that *j*, *k*, and *i* are unit vectors in the θ, *z*, and *R* orientations, respectively. Eventually, the pertained rotating system's kinetic energy would be obtained as:

$$T=T_1+T_2=\int_V\frac{1}{2}\rho\left[\left(\frac{\partial u}{\partial t}-\Omega v\right)^2+\left(\frac{\partial v}{\partial t}+\Omega(R+u)\right)^2+\left(\frac{\partial w}{\partial t}\right)^2\right]dV \tag{13}$$

The kinetic energy could be expressed as below, if spinning terms are not considered:

$$\begin{aligned}&\delta T_1=\int_V\rho\left(\frac{\partial u}{\partial t}\frac{\partial\delta u}{\partial t}+\frac{\partial v}{\partial t}\frac{\partial\delta v}{\partial t}+\frac{\partial w}{\partial t}\frac{\partial\delta w}{\partial t}\right)dV:\\&\delta T_1=\int_{R_1}^{R_2}\int_0^{\beta}\begin{bmatrix}\left\{-I_O\frac{\partial^2u_0}{\partial t^2}-I_1\frac{\partial^2u_1}{\partial t^2}\right\}\delta u_0+\left\{-I_1\frac{\partial^2u_0}{\partial t^2}-I_2\frac{\partial^2u_1}{\partial t^{2u_1}}\right\}\delta u_1\\+\left\{-I_O\frac{\partial^2v_0}{\partial t^2}-I_1\frac{\partial^2v_1}{\partial t^2}+I_3c_1\left(\frac{\partial^2v_1}{\partial t^2}+\frac{\partial^3w_0}{R\partial\beta\,\partial t^2}\right)\right\}\delta v_0\\+\left\{-I_1\frac{\partial^2v_0}{\partial t^2}-I_2\frac{\partial^2v_1}{\partial t^2}\right\}\delta v_1+\left\{-I_O\frac{\partial^2w_0}{\partial t^2}\right\}\delta w_0\end{bmatrix}RdRd\beta\end{aligned} \tag{14}$$

The kinetic energy could be defined as below, if spinning terms are considered:

$$\begin{aligned}&\delta T_2=\int_V\rho\left(\Omega\left(-v\frac{\partial\delta u}{\partial t}-\frac{\partial u}{\partial t}\delta v+(R+u)\frac{\partial\delta v}{\partial t}+\frac{\partial v}{\partial t}\delta u\right)+\left[(R+u)\delta u+v\delta v\right]\Omega^2\right)dV:\\&=\int_A\begin{pmatrix}\begin{pmatrix}\Omega\left(-\left(I_0\frac{\partial}{\partial t}v_0+I_1\frac{\partial}{\partial t}v_1\right)-\left(I_0\frac{\partial}{\partial t}v_0+I_1\frac{\partial}{\partial t}v_1\right)\right)\\-\Omega^2\left(R+I_0u_0+I_1u_1-c_1I_3\left[u_1+\frac{\partial w_0}{\partial R}\right]\right)\end{pmatrix}\delta u_0\\+\begin{pmatrix}\Omega\left(-\left(I_0\frac{\partial}{\partial t}u_0+I_1\frac{\partial}{\partial t}u_1\right)+\left(I_0\frac{\partial}{\partial t}u_0+I_1\frac{\partial}{\partial t}u_1\right)\right)\\-\Omega^2\left(I_0v_0+I_1v_1-c_1I_3\left[v_1+\frac{\partial w_0}{R\partial\beta}\right]\right)\end{pmatrix}\delta v_0\\+\begin{pmatrix}\Omega\begin{pmatrix}\left(I_0\frac{\partial^2}{\partial t\partial R}v_0+I_1\frac{\partial^2}{\partial t\partial R}v_1\right)-\left(I_0\frac{1}{R}\frac{\partial^2}{\partial t\partial\beta}u_0+I_1\frac{1}{R}\frac{\partial^2}{\partial t\partial\beta}u_1\right)\\-\left(I_0\frac{1}{R}\frac{\partial^2}{\partial t\partial\beta}u_0+I_1\frac{1}{R}\frac{\partial^2}{\partial t\partial\beta}u_1\right)+\left(I_0\frac{\partial^2}{\partial t\partial R}v_0+I_1\frac{\partial^2}{\partial t\partial R}v_1\right)\end{pmatrix}\\+\Omega^2\left(\left(I_0\frac{1}{R}\frac{\partial}{\partial\beta}v_0+I_1\frac{1}{R}\frac{\partial}{\partial\beta}v_1\right)+\left(I_0\frac{\partial}{\partial R}u_0+I_1\frac{\partial}{\partial R}u_1\right)\right)\end{pmatrix}\delta w_0\end{pmatrix}dA\\&+\begin{pmatrix}-\Omega(I_1)\left(\left(I_0\frac{\partial}{\partial t}v_0+I_1\frac{\partial}{\partial t}v_1\right)-\left(I_0\frac{\partial}{\partial t}v_0+I_1\frac{\partial}{\partial t}v_1\right)\right)\\-\Omega^2(I_1)\left(R+I_0u_0+I_1u_1\right)\end{pmatrix}\delta u_1\\+\begin{pmatrix}\Omega(I_1-c_1I_3)\left(-\left(I_0\frac{\partial}{\partial t}u_0+I_1\frac{\partial}{\partial t}u_1\right)+\left(I_0\frac{\partial}{\partial t}u_0+I_1\frac{\partial}{\partial t}u_1\right)\right)\\-\Omega^2(I_1)\left(I_0v_0+I_1v_1\right)\end{pmatrix}\delta v_1\end{aligned} \tag{15}$$

where (Safarpour *et al.* 2017, Safarpour *et al.* 2018, Al-Furjan *et al.* 2020m, n, o, p, q, r):

$$\left\{I_0,I_1,I_2,I_3\right\}=\int_{-\frac{h}{2}}^{\frac{h}{2}}\rho\left\{1,z,z^2,z^3\right\}dZ \tag{16}$$

here Ω denotes spinning velocity. Also, the current composite structure's strain energy would be derived as:

$$\begin{aligned}&\delta U=\frac{1}{2}\iiint_V\sigma_{ij}\delta\varepsilon_{ij}\,dV\\&=\int_A\begin{bmatrix}\left(N_{RR}\frac{\partial\delta u_0}{\partial R}+M_{RR}\frac{\partial\delta u_1}{\partial R}\right)\\+\left(N_{\beta\beta}\frac{\partial\delta v_0}{R\partial\beta}+M_{\beta\beta}\frac{\partial\delta v_1}{R\partial\beta}+N_{\beta\beta}\frac{\delta u_0}{R}+M_{\beta\beta}\frac{\delta u_1}{R}\right)\\+\left(N_{R\beta}\frac{\partial\delta v_0}{\partial R}+M_{R\beta}\frac{\partial\delta v_1}{\partial R}+N_{R\beta}\frac{\partial\delta u_0}{R\partial\beta}+M_{R\beta}\frac{\partial\delta u_1}{R\partial\beta}\right)\\-c_1P_{R\beta}\left[\frac{\partial\delta u_1}{R\partial\beta}+\frac{\partial^2\delta w_0}{R\partial\beta\,\partial R}\right]-N_{R\beta}\frac{\delta v_0}{R}-M_{R\beta}\frac{\delta v_1}{R}\\+\left(N_{Rz}\right)\left(\delta u_1+\frac{\partial\delta w_0}{\partial R}\right)+\left(N_{\beta z}\right)\left(\delta v_1+\frac{\partial\delta w_0}{R\partial\beta}\right)\end{bmatrix}dA\end{aligned} \tag{17}$$

which:

$$\begin{aligned}&\left\{N_{RR},M_{RR}\right\}=\int_z\left\{\sigma_{RR},z\sigma_{RR}\right\}dz;\\&\left\{N_{\beta\beta},M_{\beta\beta}\right\}=\int_z\left\{\sigma_{\beta\beta},z\sigma_{\beta\beta}\right\}dz;\\&\left\{N_{Rz},M_{Rz},Q_{Rz}\right\}=\int_z\left\{\sigma_{Rz},z\sigma_{Rz},z^2\sigma_{Rz}\right\}dz;.\\&\left\{N_{R\beta},M_{R\beta},Q_{R\beta}\right\}=\int_z\left\{\sigma_{R\beta},z\sigma_{R\beta},z^2\sigma_{R\beta}\right\}dz;\\&\left\{N_{\beta z},M_{\beta z},Q_{\beta z}\right\}=\int_z\left\{\sigma_{\beta z},z\sigma_{\beta z},z^2\sigma_{\beta z}\right\}dz.\end{aligned} \tag{18}$$

It should be mentioned that the centrifugal force which is in result of the structure's spinning feature in the may be written as (Mahinzare, Ranjbarpur *et al.* 2018; Hu and Li 2019):

$$\delta W_1=\int_A\left[\left(N^{Rotation}\right)\left(\frac{\partial w_0}{\partial R}\frac{\partial\delta w_0}{\partial R}+\frac{\partial w_0}{R^2\partial\beta}\frac{\partial\delta w_0}{\partial\beta}\right)\right]dA \tag{19}$$

where

$$N^{Rotation}=\int_{-h/2}^{h/2}\left(\frac{\rho\Omega^2}{8}(2R)(3+\nu)\right)dz \tag{20}$$

Since it is obvious from figure 1, the internal and upper composite layers are covered by viscoelastic substrate. Then, the viscoelastic foundation's work, would be obtained as:

$$\delta W_2=\int_A\left[K_w w\delta w+C_d\dot{w}\delta\dot{w}\right]dA \tag{21}$$

Ultimately, pertaining BCs and governing motion equations would be extracted using inserting Eqs. (19), (17), and (13) in the principle of minimum energy (Eq. (11)) which would be defined as:

$$\begin{aligned}&\delta u_0:\\&\frac{\partial}{\partial R}N_{RR}-\frac{N_{\beta\beta}-N_{RR}}{R}+\frac{\partial}{R\partial\beta}N_{R\beta}=I_0\frac{\partial^2u_0}{\partial t^2}+I_1\frac{\partial^2u_1}{\partial t^2}\\&+\left(\Omega\left(-\left(I_0\frac{\partial}{\partial t}v_0+I_1\frac{\partial}{\partial t}v_1\right)-\left(I_0\frac{\partial}{\partial t}v_0+I_1\frac{\partial}{\partial t}v_1\right)\right)-\Omega^2\left(R+I_0u_0+I_1u_1\right)\right)\end{aligned} \tag{22}$$

δv_0 :

$$\frac{\partial}{R\partial\beta}N_{\beta\beta}+\frac{2N_{R\beta}}{R}+\frac{\partial}{\partial R}N_{R\beta}=I_0\frac{\partial^2 v_0}{\partial t^2}+I_1\frac{\partial^2 v_1}{\partial t^2}$$
$$+\left(\Omega\left(-\left(I_0\frac{\partial}{\partial t}u_0+I_1\frac{\partial}{\partial t}u_1\right)+\left(I_0\frac{\partial}{\partial t}u_0+I_1\frac{\partial}{\partial t}u_1\right)\right)-\Omega^2\left(I_0v_0+I_1v_1\right)\right) \quad (23)$$

δw_0 :

$$\frac{\partial}{\partial R}\left(N_{Rz}\right)+\frac{\partial}{R\partial\beta}\left(N_{\beta z}\right)+\frac{\partial}{\partial R}N_{Rz}+\frac{\partial}{R\partial\beta}N_{\beta z}-N^{Rotation}\left(\frac{\partial^2 w_0}{\partial x^2}+\frac{\partial^2 w_0}{R^2\partial\beta^2}\right)$$
$$-K_w w-C_d\dot{w}=\left(I_0\frac{\partial^2 w_0}{\partial t^2}\right)$$
$$+\left(\begin{array}{l}\Omega\left(\begin{array}{l}\left(I_0\frac{\partial^2}{\partial R\partial t}v_0+I_1\frac{\partial^2}{\partial R\partial t}v_1\right)-\left(I_0\frac{1}{R}\frac{\partial^2}{\partial t\partial\beta}u_0+I_1\frac{1}{R}\frac{\partial^2}{\partial t\partial\beta}u_1\right)\\-\left(I_0\frac{1}{R}\frac{\partial^2}{\partial t\partial\beta}u_0+I_1\frac{1}{R}\frac{\partial^2}{\partial t\partial\beta}u_1\right)+\left(I_0\frac{\partial^2}{\partial t\partial R}v_0+I_1\frac{\partial^2}{\partial t\partial R}v_1\right)\end{array}\right)\\+\Omega^2\left(\left(I_0\frac{\partial}{R\partial\beta}v_0+I_1\frac{\partial}{R\partial\beta}v_1\right)+\left(I_0\frac{\partial}{\partial R}u_0+I_1\frac{\partial}{\partial R}u_1\right)\right)\end{array}\right) \quad (24)$$

δu_1 :

$$\frac{\partial}{\partial R}M_{RR}-\frac{M_{\beta\beta}-M_{RR}}{R}+\frac{\partial}{R\partial\beta}M_{R\theta\beta}-N_{Rz}=I_1\frac{\partial^2 u_0}{\partial t^2}+I_2\frac{\partial^2 u_1}{\partial t^2}$$
$$+\left(-\Omega(I_1-c_1I_3)\left(\begin{array}{l}\left(I_0\frac{\partial}{\partial t}v_0+I_1\frac{\partial}{\partial t}v_1\right)\\-\left(I_0\frac{\partial}{\partial t}v_0+I_1\frac{\partial}{\partial t}v_1\right)\end{array}\right)-\Omega^2(I_1)\left(R+I_0u_0+I_1u_1\right)\right) \quad (25)$$

δv_1 :

$$\frac{\partial}{R\partial\beta}M_{\beta\beta}+\frac{2}{R}M_{R\beta}+\frac{\partial}{\partial R}M_{R\beta}-M_{\beta z}=I_1\frac{\partial^2 v_0}{\partial t^2}+I_2\frac{\partial^2 v_1}{\partial t^2}$$
$$+\left(\begin{array}{l}\Omega(I_1)\left(-\left(I_0\frac{\partial}{\partial t}u_0+I_1\frac{\partial}{\partial t}u_1\right)+\left(I_0\frac{\partial}{\partial t}u_0+I_1\frac{\partial}{\partial t}u_1\right)\right)\\-\Omega^2(I_1)\left(I_0v_0+I_1v_1\right)\end{array}\right) \quad (26)$$

Moreover, general pertained BCs may be written as:

$$\begin{array}{lll}\delta u_0=0 & or & N_{RR}n_R+\frac{1}{R}N_{R\beta}n_\beta=0\\ \delta v_0=0 & or & N_{R\beta}n_R+\frac{1}{R}N_{\beta\beta}n_\beta=0\\ \delta w_0=0 & or & \left(\begin{array}{l}\left((N_{Rz})+N_{Rz}\right)n_R\\+\left(+(\frac{N_{\beta z}}{R})+\frac{N_{\beta z}}{R}\right)n_\beta\end{array}\right)=0\\ \delta u_1=0 & or & \left(M_{RR}\right)n_R+\left(\frac{M_{R\beta}}{R}\right)n_\beta=0\\ \delta v_1=0 & or & \left(M_{R\beta}\right)n_R+\left(\frac{M_{\beta\beta}}{R}\right)n_\beta=0\end{array} \quad (27)$$

3. Solution procedure

This section deals with a solution approach (Huang *et al.* 2019, Gholipour *et al.* 2020a, b, Pang *et al.* 2020) known as GDQM to solve the current problem's equations. In this approach the n^{th}-order derivatives of a adequately smooth function f respect to related detached points in the whole domain's range may be assumed as a linear weighted sum function of the values at each points in the all allowable input range as follows (Shu 2012):

$$\frac{\partial^n f}{\partial r^n}=\sum_{m=1}^{M}C^{(n)}{}_{j,m}\,f_{m,k} \quad (28)$$

where, $C^{(n)}$ illustrates weighting parameters for the derivative of n^{th}-order in the orientation of its radius, which would be obtained as:

$$\begin{array}{ll}C_{ij}^{(1)}=-\sum_{j=1,i\neq j}^{n}C_{ij}^{(1)} & i=j\\ C_{ij}^{(1)}=\frac{M\left(x_i\right)}{\left(x_i-x_j\right)M\left(x_j\right)} & i,j=1,2,...,\mathrm{n}\ \text{ and }\ \mathrm{i}\neq\mathrm{j}\end{array} \quad (29)$$

here,

$$M\left(x_i\right)=\prod_{j=1,j\neq i}^{n}\left(x_i-x_j\right) \quad (30)$$

Eq. (27)'s derivatives would be defined as the relations given below:

$$\begin{array}{l}C_{ii}^{(n)}=-\sum_{j=1,i\neq j}^{n}C_{ij}^{(n)}\\ 1\le n\le N-1 \text{ while } \ j,i=1,2,...,N\\ C_{ij}^{(n)}=r\left[C_{ij}^{(n-1)}C_{ij}^{(1)}-\frac{C_{ij}^{(n-1)}}{\left(x_i-x_j\right)}\right]\\ \mathrm{i}\neq\mathrm{j},2\le n\le N-1 \text{ while } \ j,i=1,2,...,N.\end{array} \quad (31)$$

Then by employing Chebyshev greed polynomials points, the seed through r-axes would be distributed as:

$$r_i=\frac{R_0-R_i}{2}\left(1-\cos\left(\frac{(i-1)}{(N_i-1)}\pi\right)\right)+R_i \qquad i=1,2,3,\ldots,N_i \quad (32)$$

However, disk's displacement fields may be written as:

$$\begin{Bmatrix}u_0(R,\beta,t)\\v_0(R,\beta,t)\\w_0(R,\beta,t)\\u_1(R,\beta,t)\\v_1(R,\beta,t)\end{Bmatrix}=\sum_{n=1}^{\infty}\begin{Bmatrix}u_{0n}(R)\times\sin(n\beta)\\v_{0n}(R)\times\cos(n\beta)\\w_{0n}(R)\times\sin(n\beta)\\u_{1n}(R)\times\sin(n\beta)\\v_{1n}(R)\times\cos(n\beta)\end{Bmatrix}e^{i\omega t} \quad (33)$$

Ultimately, the formulation of the GDQ considering BC relations may be defined as:

$$\left(\begin{bmatrix}[M_{dd}] & [M_{db}]\\ [M_{bd}] & [M_{bb}]\end{bmatrix}\omega_n^2+\begin{bmatrix}[C_{dd}] & [C_{db}]\\ [C_{bd}] & [C_{bb}]\end{bmatrix}\omega_n+\begin{bmatrix}[K_{dd}] & [K_{db}]\\ [K_{bd}] & [K_{bb}]\end{bmatrix}\right)\begin{Bmatrix}\delta_d\\ \delta_b\end{Bmatrix}=0 \quad (34)$$

Here, domain and boundary grid-points are explained by b and d, respectively. Furthermore, displacement vector are denoted by δ index. M, K, and C would be, respectively, the mass, stiffness, and damping. Then, by using Eq. (33) the novel system would be as:

$$\left[K_{db}\right]\delta_b+\left[K_{dd}\right]\delta_d=0 \quad (35a)$$

Table 1 Material properties and efficiency parameter of GPLRC structure

Graphene Platlets	E^{GPL} [Gpa] 1010	ν^{GPL} 0.186	ρ^{GPL} [kg/m^3] 1062.5	α^{GPL} [$\times10^{-6}/k$] 5	l^{GPL} [μm] 2.5	t^{GPL} [nm] 1.5	w^{GPL} [μm] 1.5
Copper matrix	E^m [Gpa] 130	ν^m 0.34	ρ^m [kg/m^3] 8960		α^m [$\times10^{-6}/k$] 17e-6		

Table 2 Comparison of the non-dimensional natural frequency of the current structure with the published article in the literature

		S-S				C-C			
	R_0/R_i	Mode number				Mode number			
		1	2	3	4	1	2	3	4
Ref. (Han and Liew 1999)	0.001	14.585	51.681	112.89	198.34	27.180	75.264	148.01	245.37
Current study	0.001	13.524	50.202	111.76	198.51	28.414	77.263	151.05	249.15
Ref. (Han and Liew 1999)	0.050	14.424	50.309	107.15	182.45	26.434	71.128	135.14	215.18
Current study	0.050	13.428	49.009	106.19	182.18	27.579	72.666	136.26	214.36
Ref. (Han and Liew 1999)	0.100	13.774	46.847	94.570	151.81	24.529	62.040	111.02	167.06
Current study	0.100	13.154	46.161	93.694	151.26	25.458	62.734	110.29	163.31
Ref. (Han and Liew 1999)	0.150	13.118	42.530	81.419	124.82	22.130	52.662	90.186	131.25
Current study	0.150	12.738	42.082	81.136	124.14	22.809	52.735	88.862	127.41
Ref. (Han and Liew 1999)	0.200	12.350	38.237	70.124	104.10	19.743	44.813	74.760	106.71
Current study	0.200	12.226	38.143	70.175	104.14	20.194	44.583	73.528	103.65

$$\left[K_{bb}\right]\delta_b+\left[K_{bd}\right]\delta_d=0 \tag{35b}$$

here, the freedom degrees' vector may explain as:

$$\delta_b=-\frac{\left[K_{dd}\right]}{\left[K_{db}\right]}\delta_d \tag{36}$$

By inserting of Eq. (35) in Eq. (34b):

$$\left(\left[K_{bd}\right]-\left[K_{bb}\right]\left[K_{db}\right]^{-1}\left[K_{dd}\right]\right)\delta_d=0 \tag{37}$$

Then

$$K^*=\left[K_{bd}\right]-\left[K_{bb}\right]\left[K_{db}\right]^{-1}\left[K_{dd}\right] \tag{38}$$

and

$$\left[C_{bd}\right]\delta_d+\left[C_{bb}\right]\delta_b=0 \tag{39}$$

By inserting Eq. (35) in Eq. (38), have:

$$\left(\left[C_{bd}\right]-\left[C_{bb}\right]\left[K_{db}\right]^{-1}\left[K_{dd}\right]\right)\delta_d=0 \tag{40}$$

Then

$$C^*=\left[C_{bd}\right]-\left[C_{bb}\right]\left[K_{db}\right]^{-1}\left[K_{dd}\right] \tag{41}$$

and

$$\left[M_{bd}\right]\delta_d+\left[M_{bb}\right]\delta_b=0 \tag{42}$$

Also, by inserting Eq. (35) in Eq. (41), have:

$$\left(\left[M_{bd}\right]-\left[M_{bb}\right]\left[K_{db}\right]^{-1}\left[K_{dd}\right]\right)\delta_d=0 \tag{43}$$

Then

$$M^*=\left[M_{bd}\right]-\left[M_{bb}\right]\left[K_{db}\right]^{-1}\left[K_{dd}\right] \tag{44}$$

Eventually, by solving the next relation, structure's displacement fields and frequency information may be derived through using GDQM.

$$K^*+M^*\omega^2+C^*\omega=0 \tag{45}$$

It could be mentioned that the non-dimensional frequency may be calculated as:

$$\bar{\omega}=\omega R_0^2\sqrt{\rho h/D},\qquad D=Eh^3/\left(12(1-\nu^2)\right) \tag{46}$$

The final goal of the current paper which is boosting disks' dynamics, would lead to introducing a famous filler, known as hybrid multi-scale nano-sized composites, although these reinforcements' thermo-mechanical properties along with epoxy's properties employed in this research are demonstrated in Table 1.

4. Validation

For examination of the current approach, the annular plate's frequency factors extracted in this scrutinization

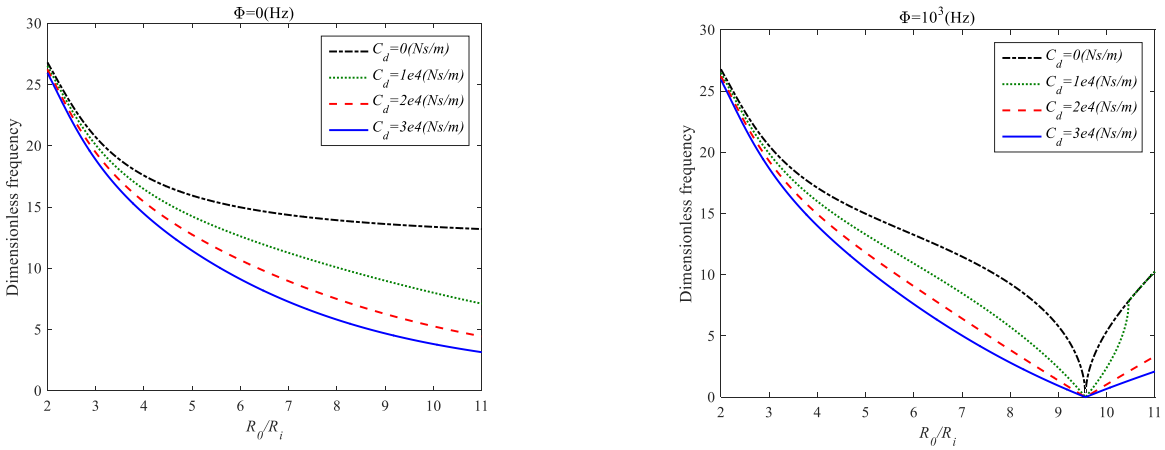

Fig. 2 The influences of C_d, Φ, R_o/R_i parameters on the frequency information of a rotating GPLs reinforced disk

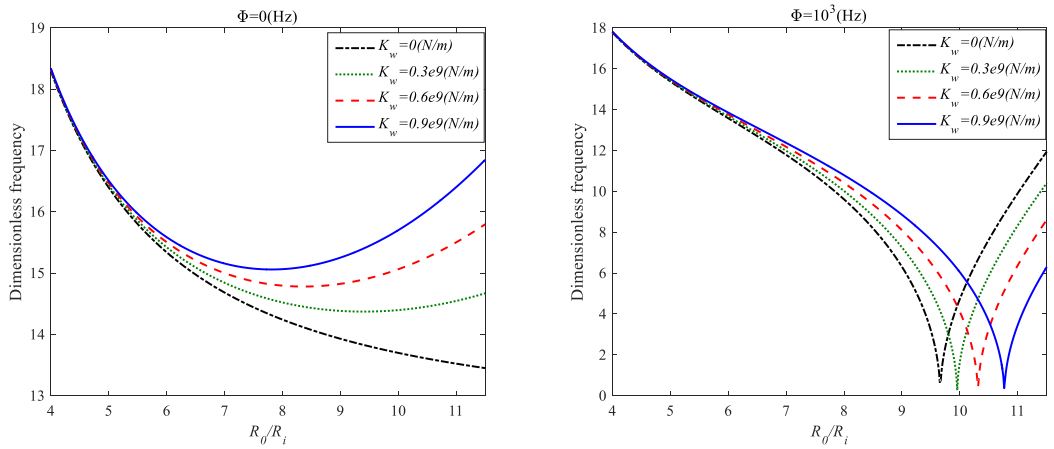

Fig. 3 The influences of K_w, Φ, R_o/R_i parameters on the frequency information of a rotating GPLs reinforced disk

are validated with those reported in Han and Liew (1999) for a wide range of axisymmetric cases of modes of vibration through the ratio of outer radius to inner radius R_0/R_i considering three different BCs as depicted in Table 2. Due to the tables reported in this paper, the present study approximates the annular plate's dynamics very much closer than those presented in Ref. (Han and Liew 1999). The system's kinematics would be explained through FSDT in Ref. (Han and Liew 1999). Moreover, it would be mentioned that the discrepancies in a couple of outcomes drop dramatically when we want to analyze higher modes of vibrations and larger values in ratios of R_0/R_i.

5. Numerical results

We present Fig. 2 for investigation of the influences of the damping parameter of the foundation (C_d), rotating speed (Φ), and radius ratio (R_o/R_i) on the frequency information of a rotating GPLs reinforced disk.

If we have attention to Fig. 2 can see that when the rotation speed is zero, the radius ratio will be a reason for ever decreasing the frequency of the structure while when $\Phi > 0$, the frequency of the disk is decreased as long as having a critical radius ratio. For better understanding, at the value of radius ratio that the frequency of the system will be zero, the critical R_o/R_i is appeared. According to above figure when the damping parameter of the foundation increases the frequency of the rotary system can improve but this matter will be seen at the higher value of radius ratio. Also, Fig. 2 prove that in the condition that $\Phi > 0$, increase in the damping parameter cannot make any change in the critical radius ratio.

Fig. 3 is candidate for having a study about the impacts of the Winkler or elastic parameter of the foundation (K_w), rotating speed (Φ), and radius ratio (R_o/R_i) on the frequency information of a rotating GPLs reinforced disk. We should attention to Fig. 3 because there is shown that if we have a rotary disk without doubt we will have critical radius ratio while a static disk does not have limitation on the R_o/R_i parameter. Generally, there is an indirect relation between the radius ratio of the composite disk and dynamic stability of the structure. As a main full result, increasing the Kw parameter cannot play an effect on the frequency of the disk at the lower value of the radius ratio while the Winkler parameter will provide an enhancement on the critical radius ratio and frequency of the GPLs reinforced disk at the higher outer radius. When the system is static or the rotational speed is zero and at the higher value of K_w, the effect of elastic foundation is overcome by

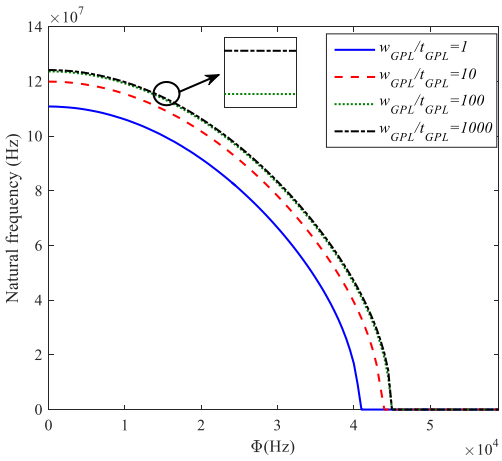

Fig. 4 Geometrical property of the GPLs and rotating speed effects on the real part of frequency of the rotary cantilevered disk

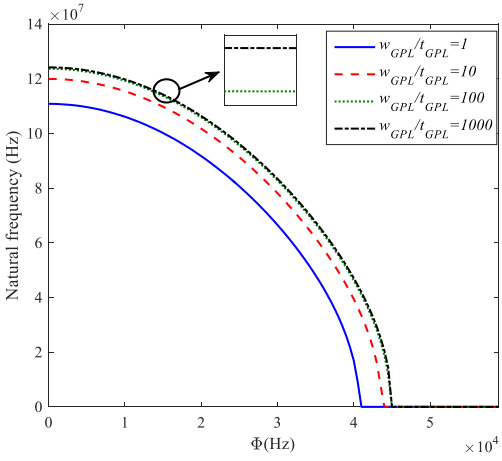

Fig. 4 Geometrical property of the GPLs and rotating speed effects on the real part of frequency of the rotary cantilevered disk

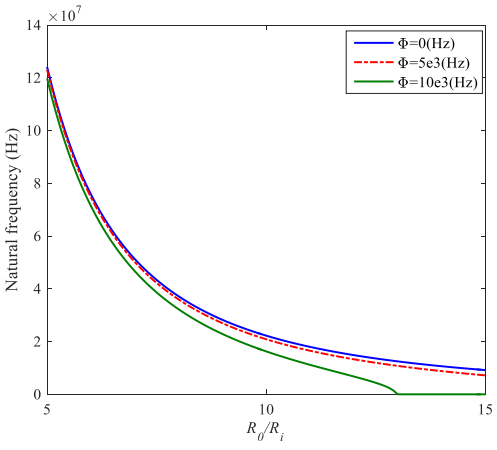

Fig. 5 Inner to outer radius ratio effect on the real part of frequency of the rotary cantilever disk for three values of the rotating speed

the radius ratio and the relation between the R_o/R_i and frequency of the system will change from indirect to direct.

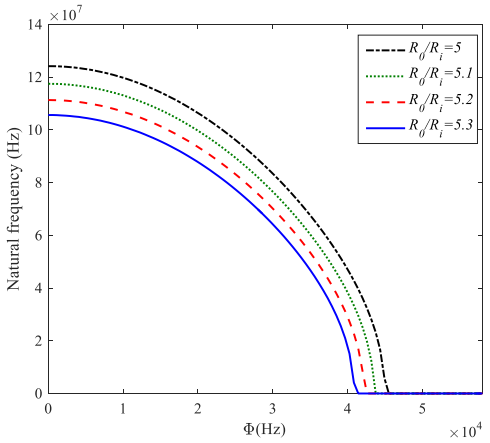

Fig. 6 Applied rotational speed effect on the real part of frequency of the rotary cantilevered disk for four values of inner to outer radius ratio

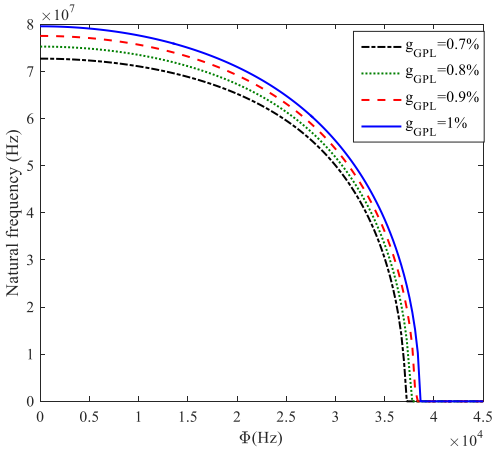

Fig. 7 Applied rotational speed influence on the real part of frequency of the rotary cantilever disk for four values of GPLs weight fraction

The given diagram in Fig. 4 evaluates the width to thickness ratio of GPLs and rotating speed effects on the frequency of the rotary cantilevered disk.

In view of Fig. 4 adding the wide GPLs in the epoxy matrix of the disk and increasing the rotating speed have direct and indirect effects on the frequency of the rotary cantilevered disk, respectively. Also, change in the high values of the geometrical information of the GPLs does not make any effect on the critical speed and the extent of the stable or instable area. Fig. 5 takes part to study the frequency of the rotary cantilever disk by considering the inner to outer radius ratio effect for three values of the rotating speed.

Fig. 5 illustrates that as long as the internal to external radius ratio and spinning velocity continue to grow, the real part frequency of the structure continues to decrease. In addition, the rotating speed effect on the real part of frequency is more effective in the higher values of the radius ratio.

Fig. 6 carries out research into the effects of inner to outer radius ratio and applied rotational speed on the frequency of the cantilevered disk. Based on the finding of

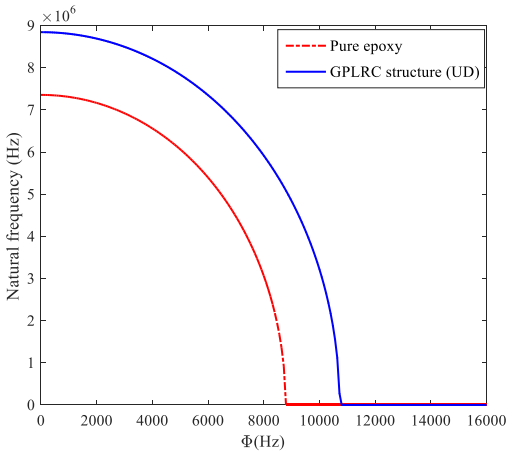

Fig. 8 Applied rotational speed effect on the real part of frequency of the rotary cantilever disk for three GPLRC patterns

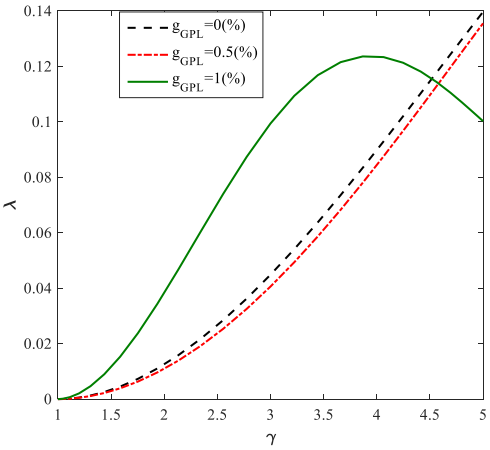

Fig. 11 x/R_i versus non-dimensional amplitude of the spinning cantilever disk for three value of g_{GPL}, pattern 2, h=0.1Ri g_{GPL}=1%, and $R0/Ri$=5

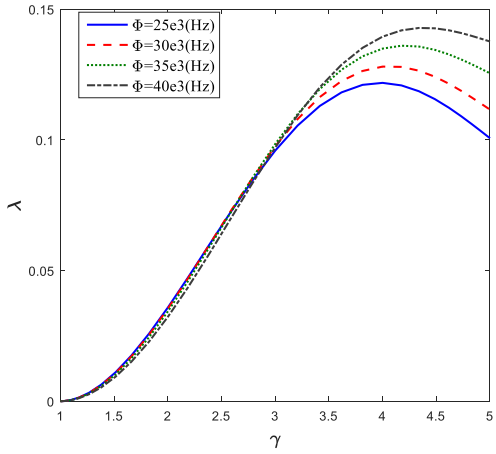

Fig. 9 x/R_i versus dimensionless amplitude of the rotary cantilever disk for four value of the external rotating speed and Pattern 4, g_{GPL}=1%, $R0/Ri$=5

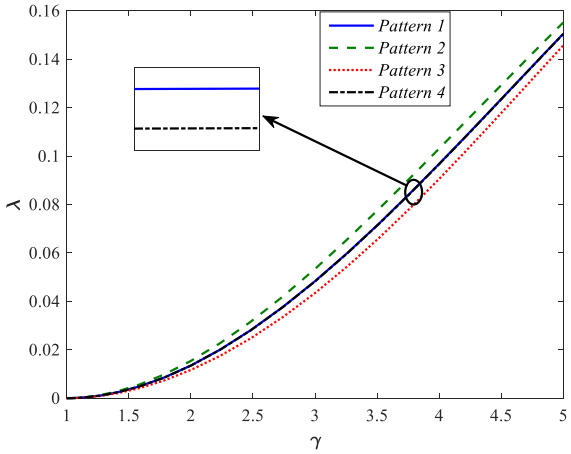

Fig. 10 γ parameter versus dimensionless amplitude of the rotary cantilever disk for four GPLRC patterns, h=0.1Ri g_{GPL}=0.05%, and $R0/Ri$=5

Fig. 6 can conclude that the rotational speed to buckle the structure and stable area of the system are rising as a result of increasing the outer radius relative to the inner radius.

Fig. 7 is intended to provide information for studying the reinforcement material percentage effect on the frequency of the cantilever disk.

The presence of Fig. 7 is essential to prove that ever-increasing the value fraction of the reinforcement provides improvements in the rotational speed to buckle the structure. Also, the stable area is expanded by having more GPLs in the matrix of the rotary cantilever disk. The good reason for this enhancement is that the structure is being harder with adding the GPLs and provides the higher critical rotating speed. As an alternative explanation, the higher the value fraction of GPLs, the better dynamic responses and the lower instable area in the system.

For the purpose of a research on the frequency of the cantilever disk with taking into account various GPLs patterns, Fig. 8 is provided.

The principal objective of figure 8 is that the best structure is GPLRC one for having a structure with the highest critical rotating speed and the widest stable area. When the structure made by pure epoxy material, the damping of the system is happened at the lowest rotating speed and the system is more ready for changing its condition from stable to instable in comparison with composite structure.

Fig. 9 conducts an analysis for providing amplitude data with attention to the inserted external spinning velocity influence on the matter. Through Fig. 9 can find out that the picked at the dimensionless amplitude ($\lambda = w/R_0$) of the structure is being far from the free edge of the disk thanks to have a decline in the value of the applied rotating speed. In other word when the applied speed reduces, the maximum amplitude can be close to inner reduce of the disk. Furthermore, for $1 \leq \gamma \leq 3$ and $3 < \gamma \leq 5$, there is an indirect and direct effect from applied rotating speed on the dimensionless amplitude of the cantilever disk.

For the purpose of having a research on the dimensionless amplitude of the cantilever disk with taking into account various GPLRC patterns, Fig. 10 is presented.

Fig. 10 shows that when the pattern 2 and pattern 3 are employed to reinforced the structure, being close to the

outer edge of the disk leads to increase and decrease in the amplitude of a cantilever disk, respectively. By considering pattern 1 and pattern 4 for reinforcing the rotary disk, the relation between the γ parameter and amplitude is equal and similar.

The given diagram in Fig. 11 evaluates the value fraction of GPLs (g_{GPL}) effect on the dimensionless amplitude of the rotary cantilever disk.

The principal objective of figure 11 is that not only there is a decline in the pick of the amplitude owning to using the more GPLs, but also an ever-increasing in the value of g_{GPL} coefficient is a reason for having the maximum amplitude far from the edge of the cantilever rotary disk.

6. Conclusions

In this paper, amplitude and vibrational behavior of a spinning cantilevered GPLRC disk covered by viscoelastic substrate have been introduced. Energy approaches have been applied for deriving the differential governing motion equations. The outcomes have been verified when it comes to contrasting them with published outcomes presented in the literature review. Despite from computational solution, an FE approach has been applied using the FE package for simulating the smart cantilevered GPLRC disk's response. The outcomes demonstrated from the FE simulation shows an excellent agreement with the semi-computational approach. The outcomes reported in this research depicted that viscoelastic substrate, angular velocity speed, GPL weight, and multifarious GPLs' patterns have a dramatic influence on the characteristics pertained to the frequency and amplitude of the spinning cantilevered GPLRC disk. The computational outcomes disclosed that:

• when the rotation speed is zero, the radius ratio will be a reason for ever decreasing the frequency of the structure while when $\Phi > 0$, the frequency of the disk is decreased as long as having a critical radius ratio.

• in the condition that $\Phi > 0$, increase in the damping parameter cannot make any change in the critical radius ratio.

• if we have a rotary disk without doubt we will have critical radius ratio while a static disk does not have limitation on the R_o/R_i parameter.

• owing to consideration of the shear correction factor via FSDT, the peaked at the rotating speed in the stable area reduces.

• change in the high values of the geometrical information of the GPLs does not make any influence on the critical velocity and the extent of the instable or stable area.

• the spinning velocity impact on the frequency is much more efficient in the higher amounts of the radius ratio.

• when the structure made by pure epoxy material, the damping of the system is happened at the lowest rotating speed and the system is more ready for changing its condition from stable to instable in comparison with composite structure.

• lowest displacement at the radial mode shape is seen for the structure when is made by pattern 2.

• As long as the radius ratio drops, the concentration of stress at the disk's internal edge would intensify.

• the picked at the dimensionless amplitude ($\lambda = w/R_0$) of the structure is being far from the free edge of the disk thanks to have a decline in the value of the inserted spinning velocity.

Acknowledgments

This work was supported by A20237.

References

Abedini, M., Mutalib, A. A., Zhang, C., Mehrmashhadi, J., Raman, S.N., Alipour, R., Momeni, T. and Mussa, M. H. (2019), "Large deflection behavior effect in reinforced concrete columns exposed to extreme dynamic loads", *Front. Struct. Civ. Eng.*, **14**(2), 532-553. https://doi.org/10.1007/s11709-020-0604-9.

Abedini, M. and Zhang, C. (2020a), "Blast performance of concrete columns retrofitted with FRP using segment pressure technique", *Compos. Struct.*, **260**, 113473. https://doi.org/10.1016/j.compstruct.2020.113473.

Abedini, M. and Zhang, C. (2020b), "Performance assessment of concrete and steel material models in ls-dyna for enhanced numerical simulation, a state of the art review", *Arch. Comput. Meth. Eng.*, 1-22. https://doi.org/10.1007/s11831-020-09483-5

Abedini, M., Zhang, C., Mehrmashhadi, J. and Akhlaghi, E. (2020c), "Comparison of ALE, LBE and pressure time history methods to evaluate extreme loading effects in RC column", *Structures*, **28**, 456-466. https://doi.org/10.1016/j.istruc.2020.08.084.

Ahmed, R.A., Fenjan, R.M. and Faleh, N.M. (2019), "Analyzing post-buckling behavior of continuously graded FG nanobeams with geometrical imperfections", *Geomech. Eng.*, **17**(2), 175-180. https://doi.org/10.12989/gae.2019.17.2.175.

Al-Furjan, M., Alzahrani, B., Shan, L., Habibi, M. and Jung, D.W. (2020a), "Nonlinear forced vibrations of nanocomposite-reinforced viscoelastic thick annular system under hygrothermal environment", *Mech. Based Des. Struct. Machines*, 1-27. https://doi.org/10.1080/15397734.2020.1824795

Al-Furjan, M., Bolandi, S.Y., Shan, L., Habibi, M. and Jung, D.W. (2020b), "On the vibrations of a high-speed rotating multi-hybrid nanocomposite reinforced cantilevered microdisk", *Mech. Based Des. Struct. Machines*, 1-29. https://doi.org/10.1080/15397734.2020.1828098.

Al-Furjan, M., Fereidouni, M., Habibi, M., Abd Ali, R., Ni, J. and Safarpour, M. (2020c), "Influence of in-plane loading on the vibrations of the fully symmetric mechanical systems via dynamic simulation and generalized differential quadrature framework", *Eng. Comput.*, 1-23. https://doi.org/10.1007/s00366-020-01177-7.

Al-Furjan, M., Habibi, M., Chen, G., Safarpour, H., Safarpour, M. and Tounsi, A. (2020d), "Chaotic oscillation of a multi-scale hybrid nano-composites reinforced disk under harmonic excitation via GDQM", *Compos. Struct.*, **252**, 112737. https://doi.org/10.1016/j.compstruct.2020.112737.

Al-Furjan, M., Habibi, M., Chen, G., Safarpour, H., Safarpour, M. and Tounsi, A. (2020e), "Chaotic simulation of the multi-phase reinforced thermo-elastic disk using GDQM", *Eng. Comput.*, 1-24. https://doi.org/10.1007/s00366-020-01144-2.

Al-Furjan, M., Habibi, M., Ebrahimi, F., Chen, G., Safarpour, M. and Safarpour, H. (2020f), "A coupled thermomechanics approach for frequency information of electrically composite microshell using heat-transfer continuum problem", *Eur. Phys.*

J. Plus, **135**(10), 1-45. https://doi.org/10.1140/epjp/s13360-020-00764-3.

Al-Furjan, M., Habibi, M., Ebrahimi, F., Mohammadi, K. and Safarpour, H. (2020g), "Wave dispersion characteristics of high-speed-rotating laminated nanocomposite cylindrical shells based on four continuum mechanics theories", *Waves Random Complex Media*, 1-27. https://doi.org/10.1080/17455030.2020.1831099.

Al-Furjan, M., Habibi, M., Ghabussi, A., Safarpour, H., Safarpour, M. and Tounsi, A. (2020h), "Non-polynomial framework for stress and strain response of the FG-GPLRC disk using three-dimensional refined higher-order theory", *Eng. Struct.*, **228**, 111496. https://doi.org/10.1016/j.engstruct.2020.111496.

Al-Furjan, M., Habibi, M. and Safarpour, H. (2020i), "Vibration control of a smart shell reinforced by graphene nanoplatelets", *Int. J. Appl. Mech.*, **12**(6), 2050066. https://doi.org/10.1142/S1758825120500660.

Al-Furjan, M., Habibi, M., won Jung, D., Chen, G., Safarpour, M. and Safarpour, H. (2020j), "Chaotic responses and nonlinear dynamics of the graphene nanoplatelets reinforced doubly-curved panel", *Eur. J. Mech. A Solids*, **85**, 104091. https://doi.org/10.1016/j.euromechsol.2020.104091.

Al-Furjan, M., Habibi, M., won Jung, D., Sadeghi, S., Safarpour, H., Tounsi, A. and Chen, G. (2020k), "A computational framework for propagated waves in a sandwich doubly curved nanocomposite panel", *Eng. Comput.*, 1-18. https://doi.org/10.1007/s00366-020-01130-8.

Al-Furjan, M., Habibi, M., won Jung, D. and Safarpour, H. (2020q), "Vibrational characteristics of a higher-order laminated composite viscoelastic annular microplate via modified couple stress theory", *Compos. Struct.*, **257**, 113152. https://doi.org/10.1016/j.compstruct.2020.113152.

Al-Furjan, M., Mohammadgholiha, M., Alarifi, I.M., Habibi, M. and Safarpour, H. (2020l), "On the phase velocity simulation of the multi curved viscoelastic system via an exact solution framework", *Eng. Comput.*, 1-17. https://doi.org/10.1007/s00366-020-01152-2.

Al-Furjan, M., Oyarhossein, M.A., Habibi, M., Safarpour, H. and Jung, D.W. (2020m), "Frequency and critical angular velocity characteristics of rotary laminated cantilever microdisk via two-dimensional analysis", *Thin-Walled Struct.*, **157**, 107111. https://doi.org/10.1016/j.tws.2020.107111.

Al-Furjan, M., Oyarhossein, M.A., Habibi, M., Safarpour, H. and Jung, D.W. (2020n), "Wave propagation simulation in an electrically open shell reinforced with multi-phase nanocomposites", *Eng. Comput.*, 1-17. https://doi.org/10.1007/s00366-020-01167-9.

Al-Furjan, M., Oyarhossein, M.A., Habibi, M., Safarpour, H., Jung, D.W. and Tounsi, A. (2020o), "On the wave propagation of the multi-scale hybrid nanocomposite doubly curved viscoelastic panel", *Compos. Struct.*, **255**, 112947. https://doi.org/10.1016/j.compstruct.2020.112947.

Al-Furjan, M., Safarpour, H., Habibi, M., Safarpour, M. and Tounsi, A. (2020p), "A comprehensive computational approach for nonlinear thermal instability of the electrically FG-GPLRC disk based on GDQ method", *Eng. Comput.*, 1-18. https://doi.org/10.1007/s00366-020-01088-7.

Al-Furjan, M.S.H., Moghadam, S.A., Dehini, R., Shan, L., Habibi, M. and Safarpour, H. (2020q), "Vibration control of a smart shell reinforced by graphene nanoplatelets under external load: Semi-numerical and finite element modeling", *Thin-Walled Struct.*, 107242. https://doi.org/10.1016/j.tws.2020.107242.

Al-Furjan, M., Dehini, R., Paknahad, M., Habibi, M. and Safarpour, H. (2021), "On the nonlinear dynamics of the multi-scale hybrid nanocomposite-reinforced annular plate under hygro-thermal environment", *Arch. Civ. Mech. Eng.*, **21**(1), 1-25. https://doi.org/10.1007/s43452-020-00151-w.

Alam, Z., Sun, L., Zhang, C., Su, Z. and Samali, B. (2020a), "Experimental and numerical investigation on the complex behaviour of the localised seismic response in a multi-storey plan-asymmetric structure", *Struct. Infrastruct. Eng.*, **17**(1), 86-102. https://doi.org/10.1080/15732479.2020.1730914.

Alam, Z., Zhang, C. and Samali, B. (2020b), "Influence of seismic incident angle on response uncertainty and structural performance of tall asymmetric structure", *Struct. Des. Tall Special Buildings*, **29**(12), e1750. https://doi.org/10.1002/tal.1750.

Alam, Z., Zhang, C. and Samali, B. (2020c), "The role of viscoelastic damping on retrofitting seismic performance of asymmetric reinforced concrete structures", *Earthq. Eng. Eng. Vib.*, **19**(1), 223-237. https://doi.org/10.1007/s11803-020-0558-x.

Atabak, R., Sedighi, H.M., Reza, A. and Mirshekari, E. (2020), "Instability analysis of bi-axial micro-scanner under electromagnetic actuation including small scale and damping effects", *Microsyst. Technol.*, 1-24. https://doi.org/10.1007/s00542-020-04802-z.

Bagheri, H., Kiani, Y. and Eslami, M. (2019), "Asymmetric compressive stability of rotating annular plates", *Eur. J. Comput. Mech.*, 1-21. https://doi.org/10.1080/17797179.2018.1560989.

Bai, B., Li, H., Zhang, W. and Cui, Y. (2020), "Application of extremum response surface method-based improved substructure component modal synthesis in mistuned turbine bladed disk", *J. Sound Vib.*, **472**, 115210. https://doi.org/10.1016/j.jsv.2020.115210.

Bisheh, H., Alibeigloo, A., Safarpour, M. and Rahimi, A. (2019), "Three-dimensional static and free vibrational analysis of graphene reinforced composite circular/annular plate using differential quadrature method", *Int. J. Appl. Mech.*, **11**(8), 1950073. https://doi.org/10.1142/S175882511950073X.

Boulefrakh, L., Hebali, H., Chikh, A., Bousahla, A.A., Tounsi, A. and Mahmoud, S. (2019), "The effect of parameters of visco-Pasternak foundation on the bending and vibration properties of a thick FG plate", *Geomech. Eng.*, **18**(2), 161-178. https://doi.org/10.12989/gae.2019.18.2.161.

Cao, L. (2020), "Changing port governance model: Port spatial structure and trade efficiency", *J. Coastal Res.*, **95**(sp1), 963-968. https://doi.org/10.2112/SI95-187.1.

Chikr, S.C., Kaci, A., Bousahla, A.A., Bourada, F., Tounsi, A., Bedia, E., Mahmoud, S., Benrahou, K.H. and Tounsi, A. (2020), "A novel four-unknown integral model for buckling response of FG sandwich plates resting on elastic foundations under various boundary conditions using Galerkin's approach", *Geomech. Eng.*, **21**(5), 471-487. https://doi.org/10.12989/gae.2020.21.5.471.

Cui, D., Li, J., Zhang, X., Zhang, L., Chang, H. and Wang, Q. "Pyrolysis temperature effect on compositions of basic nitrogen species in Huadian shale oil using positive-ion ESI FT-ICR MS and GC-NCD", *J. Anal. Appl. Pyrolysis*, **153**, 104980. https://doi.org/10.1016/j.jaap.2020.104980.

Dai, T., Dai, H.-L. and Lin, Z.-Y. (2019), "Multi-field mechanical behavior of a rotating porous FGMEE circular disk with variable thickness under hygrothermal environment", *Compos. Struct.*, **210**, 641-656. https://doi.org/10.1016/j.compstruct.2018.11.077.

De Villoria, R.G. and Miravete, A. (2007), "Mechanical model to evaluate the effect of the dispersion in nanocomposites", *Acta Materialia*, **55**(9), 3025-3031. https://doi.org/10.1016/j.actamat.2007.01.007.

Dong, Q. and Cui, L. (2021), "Reliability analysis of a system with two-stage degradation using Wiener processes with piecewise linear drift", *IMA J. Manage. Math.*, **32**(1), 3-29. https://doi.org/10.1093/imaman/dpaa009.

Dong, Q., Cui, L. and Si, S. (2020), "Reliability and availability analysis of stochastic degradation systems based on bivariate Wiener processes", *Appl. Math. Model.*, **79**, 414-433. https://doi.org/10.1016/j.apm.2019.10.044.

Ebrahimi, F., Supeni, E.E.B., Habibi, M. and Safarpour, H. (2020), "Frequency characteristics of a GPL-reinforced composite microdisk coupled with a piezoelectric layer", *Eur. Phys. J. Plus*. **135**(2), 144. https://doi.org/10.1140/epjp/s13360-020-00217-x.

El-Hassar, S.M., Benyoucef, S., Heireche, H. and Tounsi, A. (2016), "Thermal stability analysis of solar functionally graded plates on elastic foundation using an efficient hyperbolic shear deformation theory", *Geomech. Eng.*, **10**(3), 357-386. https://doi.org/10.12989/gae.2016.10.3.357.

Fahsi, A., Tounsi, A., Hebali, H., Chikh, A., Adda Bedia, E. and Mahmoud, S. (2017), "A four variable refined nth-order shear deformation theory for mechanical and thermal buckling analysis of functionally graded plates", *Geomech. Eng.*, **13**(3), 385-410. https://doi.org/10.12989/gae.2017.13.3.385.

Ghabussi, A., Ashrafi, N., Shavalipour, A., Hosseinpour, A., Habibi, M., Moayedi, H., Babaei, B. and Safarpour, H. (2019), "Free vibration analysis of an electro-elastic GPLRC cylindrical shell surrounded by viscoelastic foundation using modified length-couple stress parameter", *Mech. Based Des. Struct. Machines*, 1-25. https://doi.org/10.1080/15397734.2019.1705166.

Ghiasian, S., Kiani, Y., Sadighi, M. and Eslami, M. (2014), "Thermal buckling of shear deformable temperature dependent circular/annular FGM plates", *Int. J. Mech. Sci.*, **81**, 137-148. https://doi.org/10.1016/j.ijmecsci.2014.02.007.

Gholami, R. and Ansari, R. (2019), "On the nonlinear vibrations of polymer nanocomposite rectangular plates reinforced by graphene nanoplatelets: A unified higher-order shear deformable model", *Iran. J. Sci. Technol. Trans. Mech. Eng.*, **43**(1), 603-620. https://doi.org/10.1007/s40997-018-0182-9.

Gholipour, G., Zhang, C. and Mousavi, A.A. (2020a), "Numerical analysis of axially loaded RC columns subjected to the combination of impact and blast loads", *Eng. Struct.*, **219**, 110924. https://doi.org/10.1016/j.engstruct.2020.110924.

Gholipour, G., Zhang, C. and Mousavi, A.A. (2020b), "Nonlinear numerical analysis and progressive damage assessment of a cable-stayed bridge pier subjected to ship collision", *Mar. Struct.*, **69**, 102662. https://doi.org/10.1016/j.marstruc.2019.102662.

Gunasekaran, V., Pitchaimani, J. and Chinnapandi, L.B.M. (2020), "Analytical investigation on free vibration frequencies of polymer nano composite plate: Effect of graphene grading and non-uniform edge loading", *Mater. Today Commun.*, **24**, 100910. https://doi.org/10.1016/j.mtcomm.2020.100910.

Habibi, M., Mohammadi, A., Safarpour, H., Shavalipour, A. and Ghadiri, M. (2019), "Wave propagation analysis of the laminated cylindrical nanoshell coupled with a piezoelectric actuator", *Mech. Based Des. Struct. Machines*, 1-19. https://doi.org/10.1080/15397734.2019.1697932.

Habibi, M., Safarpour, M. and Safarpour, H. (2020), "Vibrational characteristics of a FG-GPLRC viscoelastic thick annular plate using fourth-order Runge-Kutta and GDQ methods", *Mech. Based Des. Struct. Machines*, 1-22. https://doi.org/10.1080/15397734.2020.1779086.

Han, J.B. and Liew, K. (1999), "Axisymmetric free vibration of thick annular plates", *Int. J. Mech. Sci.*, **41**(9), 1089-1109. https://doi.org/10.1016/S0020-7403(98)00057-5.

Hosseini-Hashemi, S., Es'haghi, M. and Taher, H.R.D. (2010), "An exact analytical solution for freely vibrating piezoelectric coupled circular/annular thick plates using Reddy plate theory", *Compos. Struct.*, **92**(6), 1333-1351. https://doi.org/10.1016/j.compstruct.2009.11.006.

Hu, Y. and Li, W. (2019), "Magnetoelastic axisymmetric multi-modal resonance and Hopf bifurcation of a rotating circular plate under aerodynamic load", *Nonlinear Dynam.*, **97**(2), 1295-1311. https://doi.org/10.1007/s11071-019-05049-8.

Hu, Y. and Wang, T. (2016), "Nonlinear free vibration of a rotating circular plate under the static load in magnetic field", *Nonlinear Dynam.*, **85**(3), 1825-1835. https://doi.org/10.1007/s11071-016-2798-x.

Huang, H., Huang, M., Zhang, W., Pospisil, S. and Wu, T. (2020), "Experimental investigation on rehabilitation of corroded RC columns with BSP and HPFL under combined loadings", *J. Struct. Eng.*, **146**(8), 04020157. https://doi.org/10.1061/(ASCE)ST.1943-541X.0002725.

Huang, Z., Yi, S., Chen, H. and He, X. (2019), "Parameter analysis of damaged region for laminates with matrix defects", *J. Sandw. Struct. Mater.*, 1099636219842290. https://doi.org/10.1177/1099636219842290.

Issad, M.N., Fekrar, A., Bakora, A., Bessaim, A. and Tounsi, A. (2018), "Free vibration and buckling analysis of orthotropic plates using a new two variable refined plate theory", *Geomech. Eng.*, **15**(1), 711-719. https://doi.org/10.12989/gae.2018.15.1.711.

Jafari Fesharaki, J. and Roghani, M. (2019), "Elastic behavior of functionally graded two tangled circles chamber", *J. Appl. Comput. Mech.*, **5**(4), 667-679. https://doi.org/10.22055/JACM.2019.27058.1372.

Javani, M., Kiani, Y. and Eslami, M. (2020), "Thermal buckling of FG graphene platelet reinforced composite annular sector plates", *Thin-Walled Struct.*, **148**, 106589. https://doi.org/10.1016/j.tws.2019.106589.

Ju, Y., Shen, T. and Wang, D. (2020), "Bonding behavior between reactive powder concrete and normal strength concrete", *Construct. Build. Mater.*, **242**, 118024. https://doi.org/10.1016/j.conbuildmat.2020.118024.

Karami, B., Shahsavari, D., Janghorban, M. and Tounsi, A. (2019), "Resonance behavior of functionally graded polymer composite nanoplates reinforced with graphene nanoplatelets", *Int. J. Mech. Sci.*, **156**, 94-105. https://doi.org/10.1016/j.ijmecsci.2019.03.036.

Kordestani, H. and Zhang, C. (2020), "Direct use of the savitzky–golay filter to develop an output-only trend line-based damage detection method", *Sensors*, **20**(7), 1983. https://doi.org/10.3390/s20071983.

Li, C., Sun, L., Xu, Z., Wu, X., Liang, T. and Shi, W. (2020), "Experimental investigation and error analysis of high precision FBG displacement sensor for structural health monitoring", *Int. J. Struct. Stabil. Dynam.*, **20**(6), 2040011. https://doi.org/10.1142/S0219455420400118.

Liu, D., Li, Z., Kitipornchai, S. and Yang, J. (2019), "Three-dimensional free vibration and bending analyses of functionally graded graphene nanoplatelets-reinforced nanocomposite annular plates", *Compos. Struct.*, **229**, 111453. https://doi.org/10.1016/j.compstruct.2019.111453.

Liu, C., Deng, X., Liu, J., Peng, T., Yang, S. and Zheng, Z. (2020a), "Dynamic response of saddle membrane structure under hail impact", *Eng. Struct.*, **214**, 110597. https://doi.org/10.1016/j.engstruct.2020.110597.

Liu, C., Wang, F., Deng, X., Pang, S., Liu, J., Wu, Y. and Xu, Z. (2020b), "Hailstone-induced dynamic responses of pretensioned umbrella membrane structure", *Adv. Struct. Eng.*, **24**(1), 3-16. https://doi.org/10.1177/1369433220940149.

Liu, C., Wang, F., He, L., Deng, X., Liu, J. and Wu, Y. (2020c), "Experimental and numerical investigation on dynamic responses of the umbrella membrane structure excited by heavy rainfall", *J. Vib. Control*, 1077546320932691. https://doi.org/10.1177/1077546320932691.

Liu, J., Wu, C., Wu, G. and Wang, X. (2015), "A novel differential

search algorithm and applications for structure design", *Appl. Math. Comput.*, **268**, 246-269. https://doi.org/10.1016/j.amc.2015.06.036.

Liu, J., Liu, Y. and Wang, X. (2020d), "An environmental assessment model of construction and demolition waste based on system dynamics: A case study in Guangzhou", *Environ. Sci. Pollut. Res.*, **27**(30), 37237-37259. https://doi.org/10.1007/s11356-019-07107-5.

Liu, J., Yi, Y. and Wang, X. (2020e), "Exploring factors influencing construction waste reduction: A structural equation modeling approach", *J. Clean. Prod.*, **276**, 123185. https://doi.org/10.1016/j.jclepro.2020.123185.

Long, Q., Wu, C. and Wang, X. (2015), "A system of nonsmooth equations solver based upon subgradient method", *Appl. Math. Comput.*, **251**, 284-299. https://doi.org/10.1016/j.amc.2014.11.064.

Lori, E.S., Ebrahimi, F., Supeni, E.E.B., Habibi, M. and Safarpour, H. (2020), "The critical voltage of a GPL-reinforced composite microdisk covered with piezoelectric layer", *Eng. Comput.*, 1-20. https://doi.org/10.1007/s00366-020-01004-z.

Mahinzare, M., Ranjbarpur, H. and Ghadiri, M. (2018), "Free vibration analysis of a rotary smart two directional functionally graded piezoelectric material in axial symmetry circular nanoplate", *Mech. Syst. Signal Pr.*, **100**, 188-207. https://doi.org/10.1016/j.ymssp.2017.07.041.

Moayedi, H., Aliakbarlou, H., Jebeli, M., Noormohammadiarani, O., Habibi, M., Safarpour, H. and Foong, L. (2020), "Thermal buckling responses of a graphene reinforced composite micropanel structure", *Int. J. Appl. Mech.*, **12**(01), 2050010. https://doi.org/10.1142/S1758825120500106.

Mohammad-Rezaei Bidgoli, E. and Arefi, M. (2019), "Free vibration analysis of micro plate reinforced with functionally graded graphene nanoplatelets based on modified strain-gradient formulation", *J. Sandw. Struct. Mater.*, 1099636219839302. https://doi.org/10.1177/1099636219839302.

Mohseni, A. and Shakouri, M. (2020), "Natural frequency, damping and forced responses of sandwich plates with viscoelastic core and graphene nanoplatelets reinforced face sheets", *J. Vib. Control.*, 1077546319893453. https://doi.org/10.1177/1077546319893453.

Moraveji Tabasi, H., Eskandari Jam, J., Malekzadeh Fard, K. and Heydari Beni, M. (2020), "Buckling and free vibration analysis of fiber metal-laminated plates resting on partial elastic foundation", *J. Appl. Comput. Mech.*, **6**(1), 37-51. https://doi.org/10.22055/JACM.2019.28156.1489.

Mousavi, A.A., Zhang, C., Masri, S.F. and Gholipour, G. (2020), "Structural damage localization and quantification based on a CEEMDAN hilbert transform neural network approach: A model steel truss bridge case study", *Sensors*, **20**(5), 1271. https://doi.org/10.3390/s20051271.

Ouakad, H.M. and Sedighi, H.M. (2019), "Static response and free vibration of MEMS arches assuming out-of-plane actuation pattern", *Int. J. Non-Linear Mech.*, **110**, 44-57. https://doi.org/10.1016/j.ijnonlinmec.2018.12.011.

Pang, R., Xu, B., Kong, X. and Zou, D. (2018), "Seismic fragility for high CFRDs based on deformation and damage index through incremental dynamic analysis", *Soil Dyn. Earthq. Eng.*, **104**, 432-436. https://doi.org/10.1016/j.soildyn.2017.11.017

Pang, R., Xu, B., Zhou, Y., Zhang, X. and Wang, X. (2020), "Fragility analysis of high CFRDs subjected to main shock-aftershock sequences based on plastic failure", *Eng. Struct.*, **206**, 110152. https://doi.org/10.1016/j.engstruct.2019.110152.

Qin, Z., Yang, Z., Zu, J. and Chu, F. (2018), "Free vibration analysis of rotating cylindrical shells coupled with moderately thick annular plates", *Int. J. Mech. Sci.*, **142**, 127-139. https://doi.org/10.1016/j.ijmecsci.2018.04.044.

Rabhi, M., Benrahou, K.H., Kaci, A., Houari, M.S.A., Bourada, F., Bousahla, A.A., Tounsi, A., Bedia, E.A., Mahmoud, S. and Tounsi, A. (2020), "A new innovative 3-unknowns HSDT for buckling and free vibration of exponentially graded sandwich plates resting on elastic foundations under various boundary conditions", *Geomech. Eng.*, **22**(2), 119. https://doi.org/10.12989/gae.2020.22.2.119.

Sadoun, M., Houari, M.S.A., Bakora, A., Tounsi, A., Mahmoud, S. and Alwabli, A.S. (2018), "Vibration analysis of thick orthotropic plates using quasi 3D sinusoidal shear deformation theory", *Geomech. Eng.*, **16**(2), 141-150. https://doi.org/10.12989/gae.2018.16.2.141.

Safarpour, H., Mohammadi, K. and Ghadiri, M. (2017), "Temperature-dependent vibration analysis of a FG viscoelastic cylindrical microshell under various thermal distribution via modified length scale parameter: A numerical solution", *J. Mech. Behavior Mater.*, **26**(1-2), 9-24. https://doi.org/10.1515/jmbm-2017-0010.

Safarpour, H., Mohammadi, K., Ghadiri, M. and Barooti, M.M. (2018), "Effect of porosity on flexural vibration of CNT-reinforced cylindrical shells in thermal environment using GDQM", *Int. J. Struct. Stabil. Dynam.*, **18**(10), 1850123. https://doi.org/10.1142/S0219455418501237.

Safarpour, M., Ghabussi, A., Ebrahimi, F., Habibi, M. and Safarpour, H. (2020), "Frequency characteristics of FG-GPLRC viscoelastic thick annular plate with the aid of GDQM", *Thin-Walled Struct.*, **150**, 106683. https://doi.org/10.1016/j.tws.2020.106683.

Safarpour, M., Rahimi, A. and Alibeigloo, A. (2019), "Static and free vibration analysis of graphene platelets reinforced composite truncated conical shell, cylindrical shell, and annular plate using theory of elasticity and DQM", *Mech. Based Des. Struct. Machines*, **48**(4), 496-524. https://doi.org/10.1080/15397734.2019.1646137.

Sedighi, H.M. (2020), "Divergence and flutter instability of magneto-thermo-elastic C-BN hetero-nanotubes conveying fluid", *Acta Mechanica Sinica*, **36**(2), 381-396. https://doi.org/10.1007/s10409-019-00924-4.

Sedighi, H.M. and Daneshmand, F. (2014), "Nonlinear transversely vibrating beams by the homotopy perturbation method with an auxiliary term", *J. Appl. Comput. Mech.*, **1**(1), 1-9. https://doi.org/10.22055/jacm.2014.10545.

Sedighi, H.M., Ouakad, H.M., Dimitri, R. and Tornabene, F. (2020), "Stress-driven nonlocal elasticity for the instability analysis of fluid-conveying C-BN hybrid-nanotube in a magneto-thermal environment", *Physica Scripta*, **95**(6), 065204. https://doi.org/10.1088/1402-4896/ab793f/meta.

Shokrgozar, A., Ghabussi, A., Ebrahimi, F., Habibi, M. and Safarpour, H. (2020), "Viscoelastic dynamics and static responses of a graphene nanoplatelets-reinforced composite cylindrical microshell", *Mech. Based Des. Struct. Machines*, 1-28. https://doi.org/10.1080/15397734.2020.1719509.

Shu, C. (2012), *Differential Quadrature and its Application in Engineering*, Springer Science & Business Media

Song, M., Kitipornchai, S. and Yang, J. (2017), "Free and forced vibrations of functionally graded polymer composite plates reinforced with graphene nanoplatelets", *Compos. Struct.*, **159**, 579-588. https://doi.org/10.1016/j.compstruct.2016.09.070.

Song, M., Li, X., Kitipornchai, S., Bi, Q. and Yang, J. (2019), "Low-velocity impact response of geometrically nonlinear functionally graded graphene platelet-reinforced nanocomposite plates", *Nonlinear Dynam.*, **95**(3), 2333-2352. https://doi.org/10.1007/s11071-018-4695-y.

Sun, L., Li, C., Zhang, C., Liang, T. and Zhao, Z. (2019), "The strain transfer mechanism of fiber bragg grating sensor for extra large strain monitoring", *Sensors*, **19**(8), 1851. https://doi.org/10.3390/s19081851.

Sun, L., Yang, Z., Jin, Q. and Yan, W. (2020), "Effect of axial compression ratio on seismic behavior of GFRP reinforced concrete columns", *Int. J. Struct. Stabil. Dynam.*, **20**(06), 2040004. https://doi.org/10.1142/S0219455420400040.

Tran, T.T., Tran, V.K., Le, P.B., Phung, V.M., Do, V.T. and Nguyen, H.N. (2020), "Forced vibration analysis of laminated composite shells reinforced with graphene nanoplatelets using finite element method", *Adv. Civ. Eng.* https://doi.org/10.1155/2020/1471037.

Wang, J., Lu, S., Wang, Y., Li, C. and Wang, K. (2020a), "Effect analysis on thermal behavior enhancement of lithium-ion battery pack with different cooling structures", *J. Energy Storage*. **32** 101800. https://doi.org/10.1016/j.est.2020.101800.

Wang, Q., Liu, B. and Wang, Z. (2020b), "Investigation of heat transfer mechanisms among particles in horizontal rotary retorts", *Powder Technol.*, **367**, 82-96. https://doi.org/10.1016/j.powtec.2020.03.042.

Wang, Y., Zeng, R. and Safarpour, M. (2020c), "Vibration analysis of FG-GPLRC annular plate in a thermal environment", *Mech. Based Des. Struct. Machines*, 1-19. https://doi.org/10.1080/15397734.2020.1719508.

Wu, C., Wu, P., Wang, J., Jiang, R., Chen, M. and Wang, X. (2021), "Ontological knowledge base for concrete bridge rehabilitation project management", *Automat. Constr.*, **121**, 103428. https://doi.org/10.1016/j.autcon.2020.103428.

Wu, H., Zhu, J., Kitipornchai, S., Wang, Q., Ke, L.L. and Yang, J. (2020), "Large amplitude vibration of functionally graded graphene nanocomposite annular plates in thermal environments", *Compos. Struct.*, **239**, 112047. https://doi.org/10.1016/j.compstruct.2020.112047.

Wu, T., Cao, J., Xiong, L. and Zhang, H. (2019), "New stabilization results for semi-Markov chaotic systems with fuzzy sampled-data control", *Complexity*. https://doi.org/10.1155/2019/7875305.

Xiong, L., Zhang, H., Li, Y. and Liu, Z. (2016), "Improved stability and H∞ performance for neutral systems with uncertain Markovian jump", *Nonlinear Anal. Hybrid Syst.*, **19**, 13-25. https://doi.org/10.1016/j.nahs.2015.07.005

Xu, B., Pang, R. and Zhou, Y. (2020), "Verification of stochastic seismic analysis method and seismic performance evaluation based on multi-indices for high CFRDs", *Eng. Geol.*, **264**, 105412. https://doi.org/10.1016/j.enggeo.2019.105412.

Yang, B., Kitipornchai, S., Yang, Y.F. and Yang, J. (2017), "3D thermo-mechanical bending solution of functionally graded graphene reinforced circular and annular plates", *Appl. Math. Model.*, **49**, 69-86. https://doi.org/10.1016/j.apm.2017.04.044.

Yang, Z., Xu, P., Wei, W., Gao, G., Zhou, N. and Wu, G. (2020), "Influence of the crosswind on the pantograph arcing dynamics", *IEEE T. Plasma Sci.*, **48**(8), 2822-2830. https://doi.org/10.1109/TPS.2020.3010553.

Younsi, A., Tounsi, A., Zaoui, F.Z., Bousahla, A.A. and Mahmoud, S. (2018), "Novel quasi-3D and 2D shear deformation theories for bending and free vibration analysis of FGM plates", *Geomech. Eng.*, **14**(6), 519-532. https://doi.org/10.12989/gae.2018.14.6.519.

Zhang, C., Alam, Z., Sun, L., Su, Z. and Samali, B. (2019a), "Fibre Bragg grating sensor-based damage response monitoring of an asymmetric reinforced concrete shear wall structure subjected to progressive seismic loads", *Struct. Control Health Monit.*, **26**(3), e2307. https://doi.org/10.1002/stc.2307.

Zhang, C., Gholipour, G. and Mousavi, A.A. (2019b), "Nonlinear dynamic behavior of simply-supported RC beams subjected to combined impact-blast loading", *Eng. Struct.*, **181**, 124-142. https://doi.org/10.1016/j.engstruct.2018.12.014.

Zhang, C. and Wang, H. (2019c), "Robustness of the active rotary inertia driver system for structural swing vibration control subjected to multi-type hazard excitations", *Appl. Sci.*, **9**(20), 4391. https://doi.org/10.3390/app9204391.

Zhang, C. and Wang, H. (2019d), "Swing vibration control of suspended structure using active rotary inertia driver system: Parametric analysis and experimental verification", *Appl. Sci.*, **9**(15), 3144. https://doi.org/10.3390/app9153144.

Zhang, C., Abedini, M. and Mehrmashhadi, J. (2020a), "Development of pressure-impulse models and residual capacity assessment of RC columns using high fidelity Arbitrary Lagrangian-Eulerian simulation", *Eng. Struct.*, **224**, 111219. https://doi.org/10.1016/j.engstruct.2020.111219.

Zhang, C., Gholipour, G. and Mousavi, A.A. (2020b), "State-of-the-art review on responses of RC structures subjected to lateral impact loads", *Arch. Comput. Meth. Eng.*, 1-31. https://doi.org/10.1007/s11831-020-09467-5.

Zhang, C. and Wang, H. (2020c), "Swing vibration control of suspended structures using the Active Rotary Inertia Driver system: Theoretical modeling and experimental verification", *Struct. Control Health Monit.*, **27**(6), e2543. https://doi.org/10.1002/stc.2543.

Zhang, S., Pak, R.Y. and Zhang, J. (2020d), "Vertical time-harmonic coupling vibration of an impermeable, rigid, circular plate resting on a finite, poroelastic soil layer", *Acta Geotechnica*. 1-25. https://doi.org/10.1007/s11440-020-01067-8.

Zhang, S., Zhang, J., Ma, Y. and Pak, R.Y. (2020e), "Vertical dynamic interactions of poroelastic soils and embedded piles considering the effects of pile-soil radial deformations", *Soils Found.*, **61**(1), 16-34. https://doi.org/10.1016/j.sandf.2020.10.003.

Zhang, Z., Luo, C. and Zhao, Z. (2020f), "Application of probabilistic method in maximum tsunami height prediction considering stochastic seabed topography", *Nat. Hazards*, **104**(3), 2511-2530. https://doi.org/10.1007/s11069-020-04283-3.

Zheng, J., Zhang, C. and Li, A. (2020g), "Experimental investigation on the mechanical properties of curved metallic plate dampers", *Appl. Sci.*, **10**(1), 269. https://doi.org/10.3390/app10010269.

Zhu, J., Shi, Q., Wu, P., Sheng, Z. and Wang, X. (2018), "Complexity analysis of prefabrication contractors' dynamic price competition in mega projects with different competition strategies", *Complexity*. https://doi.org/10.1155/2018/5928235.

Zhu, L., Kong, L. and Zhang, C. (2020), "Numerical study on hysteretic behaviour of horizontal-connection and energy-dissipation structures developed for prefabricated shear walls", *Appl. Sci.*, **10**(4), 1240. https://doi.org/10.3390/app10041240.

Zhu, L., Zhang, C., Guan, X., Uy, B., Sun, L. and Wang, B. (2018), "The multi-axial strength performance of composited structural BCW members subjected to shear forces", *Steel Compos. Struct.*, **27**(1), 75-87. https://doi.org/10.12989/scs.2018.27.1.075.

Zuo, C., Chen, Q., Gu, G., Feng, S., Feng, F., Li, R. and Shen, G. (2013), "High-speed three-dimensional shape measurement for dynamic scenes using bi-frequency tripolar pulse-width-modulation fringe projection", *Opt. Laser. Eng.*, **51**(8), 953-960. https://doi.org/10.1016/j.optlaseng.2013.02.012.

CC